This is the accepted manuscript (postprint) of the following article:
M. Mirak, M. Alizadeh, E. Salahinejad, R. Amini, *Zn–HA–TiO_2 nanocomposite coatings electrodeposited on a NiTi shape memory alloy*, Surface and Interface Analysis, 47 (2015) 176-183.
https://doi.org/10.1002/sia.5678

Zn-HA-TiO_2 nanocomposite coatings electrodeposited on a NiTi shape memory alloy

Mohammad Mirak [a], Morteza Alizadeh [a,*], Erfan Salahinejad [b], Rasool Amini [a]

[a] Department of Materials Science and Engineering, Shiraz University of Technology, Modarres Blvd., 71555-313, Shiraz, Iran

[b] Faculty of Materials Science and Engineering, K.N. Toosi University of Technology, Tehran, Iran

Abstract

In this work, zinc-hydroxyapatite (Zn-HA) and zinc-hydroxyapatite-titania (Zn-HA-TiO_2) nanocomposite coatings were electrodeposited onto a NiTi shape memory alloy, using a chloride zinc plating bath. The structure of the composite coatings was characterized by X-ray diffraction, scanning electron microscopy, and high-resolution transmission electron microscopy. According to the results, the Zn-HA-TiO_2 coating exhibited a plate–like surface morphology, where the addition of the nanoparticles caused to an increase in roughness. It was also found that due to applying a proper stirring procedure during co-deposition, a homogenous dispersion of the nanoparticles in the coatings was achieved. Also, the addition of the TiO_2 nanoparticles to the Zn-HA-TiO_2 coating enhanced the microhardness and wear resistance.

Keywords: Composite coatings; Electrodeposition; Structure; Biomedical applications

*Corresponding Author: *Email address:* alizadeh@sutech.ac.ir (Morteza Alizadeh)

This is the accepted manuscript (postprint) of the following article:
M. Mirak, M. Alizadeh, E. Salahinejad, R. Amini, *Zn–HA–TiO_2 nanocomposite coatings electrodeposited on a NiTi shape memory alloy*, Surface and Interface Analysis, 47 (2015) 176-183.
https://doi.org/10.1002/sia.5678

1. Introduction

During the recent decades, the development of protective coatings has attracted great attention, in order to enhance the life span of materials which face limitations during operation. These limitations strongly relate to interactions between external factors and operating environment. Zinc (Zn) is widely used as an engineering material in coatings. Zn coatings act both as a physical barrier from the surrounding corrosive environment and as an anodically protective layer. Nevertheless, if there is an enormous difference in the electronegativity of Zn and substrate, a rapid dissolution of Zn occurs under corrosive conditions, which reduces the pure Zn coating lifetime [1].

Recently, some researchers have focused on the improvement of Zn coating properties by adding ceramic nanoparticles to the coating. It has been reported that the incorporation of nanoparticles, such as TiO_2, Al_2O_3 and ZrO_2 can improve properties, particularly hardness, wear and corrosion resistance [2-4]. For instance, Venkatesha et al. [5] successfully produced Zn/TiO_2 nanocomposite coatings and showed that the microhardness and wear resistance of the Zn/TiO_2 composite coatings are improved by adding TiO_2 nanoparticles into the coatings.

Zn and TiO_2 nanoparticles are widely used in biomedical coatings [6,7]. Zn is an important component in the human bone and plays a varied role in biological functions, such as DNA synthesis, enzyme activity, nucleic acid metabolism, biomineralization, and hormonal activity [8, 9]. In addition, TiO_2 has a good biocompatibility and the existence of TiO_2 nanoparticles in coatings can ensure that the implant coating displays a good corrosion resistance in corrosive bio-fluid environment [10-12]. In addition to TiO_2, hydroxyapatite (HA) as a ceramic material is widely used in biocoatings [13-15]. HA, as a main inorganic part of natural bone, induces the highest osteoblast cell attachment and leads to a better integration of the implant [16, 17]. However, it has been recognized that HA is a brittle

This is the accepted manuscript (postprint) of the following article:
M. Mirak, M. Alizadeh, E. Salahinejad, R. Amini, *Zn–HA–TiO_2 nanocomposite coatings electrodeposited on a NiTi shape memory alloy*, Surface and Interface Analysis, 47 (2015) 176-183.
https://doi.org/10.1002/sia.5678

structure and its mechanical strength is low to be used in load-bearing applications [18]. Also, interfacial adhesion between the substrate and HA coating is relatively weak, so that it cannot be directly employed as a coating material on implants [19, 20]. Based on the increased adhesion between the substrate and coating, the foreword of layers seem to be constructive for establishing composite biocoatings on medical metals [21]. Wen et al. [8] have reported that TiO_2/HA composite coatings caused to an increased corrosion resistance. Also, Mangalaraj et al. [22] reported that the addition of TiO_2 to HA improved mechanical properties.

There are several techniques to produce composite coatings, such as physical vapor deposition, chemical vapor deposition, laser beam deposition, ion implantation, plasma jet, and electrodeposition [23-29]. Among these techniques, electrodeposition has proved itself as an efficient method through producing smoother surfaces and strong bonding between particles and metal, having the potential for a straightforward control of the coating thickness and for depositing different alloys and composite coatings, and suitability for automation [30]. The aim of this work is the synthesis of Zn-HA and Zn-HA-TiO_2 nanocomposite coatings on a NiTi shape memory alloy (SMA) by the electrodeposition method, as a candidate for biocoatings. The effects of various TiO_2 and HA nanoparticle contents on the morphology, microhardness, and wear behavior of the nanocomposite coatings were also examined.

2. Experimental procedures

2.1. Electrode pre-treatment

This is the accepted manuscript (postprint) of the following article:
M. Mirak, M. Alizadeh, E. Salahinejad, R. Amini, *Zn–HA–TiO_2 nanocomposite coatings electrodeposited on a NiTi shape memory alloy*, Surface and Interface Analysis, 47 (2015) 176-183.
https://doi.org/10.1002/sia.5678

A graphite plate was used as the anode. The cathode was a Ni-49.2 at.% Ti plate with the size of 20 mm × 16 mm × 1.5 mm. Before each electrodeposition process, the substrates were mechanically polished with emery papers to 2000, then sonicated in acetone for about 10 min, and then activated in an acid solution (15 ml HNO_3 + 5 ml HF + 80 ml H_2O) for about 1 min at room temperature. The electrodeposition process was carried out in a two-electrode equipped cell.

2.2. Electrolyte preparation and optimization

A large number of attempts were made to determine the optimum bath composition and conditions for electrodeposition of Zn-HA and Zn-HA-TiO_2 layers. The composition of the electrolyte bath was based on a modified acid chloride zinc plating bath, as listed in Table 1. The solution was prepared from analytic grade chemicals and double distilled water. The average size of TiO_2 (purity >99.9%) and HA particles was estimated to be about 40 and 80 nm, respectively. The HA and TiO_2 particles in different concentrations (0-25 gl^{-1}) were added to the bath with the same ratio. A surfactant was added in order to uniformly distribute the deposited zinc. Before electrodeposition, the electrolyte bath was stirred for about 24 h by using a magnetic stirrer at 1200 rpm for the better de-agglomeration of the HA and TiO_2 nanoparticles. Magnetic stirring was also employed to keep the particles in suspension during the composite deposition process. Both of the electrodes were dipped in 500 ml of the test electrolyte.

2.3. Microstructural and mechanical characterization

A scanning electron microscope (SEM, Vega-XMU) was employed to investigate the surface morphology of the electrodeposited Zn-HA and Zn-HA-TiO_2 coatings. The

This is the accepted manuscript (postprint) of the following article:
M. Mirak, M. Alizadeh, E. Salahinejad, R. Amini, *Zn–HA–TiO_2 nanocomposite coatings electrodeposited on a NiTi shape memory alloy*, Surface and Interface Analysis, 47 (2015) 176-183.
https://doi.org/10.1002/sia.5678

composition of the coatings was also evaluated by an energy dispersive X-ray (EDX) apparatus attached to the SEM. The EDX analysis was performed on the Zn-HA and Zn-HA-TiO_2 samples over three uniform regions. The crystal structures of the composite coatings were examined using X-ray diffraction (XRD) by a D8 Bruker diffractometer with Cu $K\alpha_1$ radiation (λ = 0.15406 nm) in the range of 2θ = 20-100° using a step size of 0.05° and a counting time of 3s per step. Finally, the microstructure and texture of the coatings were determined by a high resolution transmission electron microscope (HRTEM, FEI, Tecnai G2 F30).

The microhardness of the nanocomposite coatings was measured by a microhardness tester (Wolpert Wilson) at a load of 100 g for 15s. Five measurements were conducted on the coating cross sections and the average of the results was expressed. Wear tests were also performed at room temperature by a ball-on-disc type tribometer with a constant rotation speed of 200 rpm at a constant radius of 2.5 mm and a load of 1 N, under non-lubricated conditions. The weight loss of the samples, with an accuracy of 0.1 mg, was determined to evaluate the wear resistance.

3. Results and discussion

3.1. XRD analyses

Fig. 1 shows the XRD patterns of the Zn-HA and Zn-HA-TiO_2 nanocomposite coatings deposited on the NiTi SMA at a current density of 1 Adm^{-2}.The XRD pattern indicates that the majority of diffraction lines are related to Zn. As can be seen, both of the Zn-HA and Zn-HA-TiO_2 composite coatings exhibit the eight reflections of the Zn matrix with a hexagonal crystal structure. The deposition of Zn from the electrolyte bath results in crystallite growth predominantly in the direction of the (101) plane in the Zn-HA and Zn-HA-TiO_2 coatings.

This is the accepted manuscript (postprint) of the following article:
M. Mirak, M. Alizadeh, E. Salahinejad, R. Amini, *Zn–HA–TiO_2 nanocomposite coatings electrodeposited on a NiTi shape memory alloy*, Surface and Interface Analysis, 47 (2015) 176-183.
https://doi.org/10.1002/sia.5678

The relative intensity of the diffraction peak of the Zn (101) plane is higher than that of the other crystal planes of Zn in both of the compositions. This result suggests that the [101] axis of Zn crystals was oriented perpendicular to the specimen surface and/or that Zn crystals grew along the [101] direction. A study published on electrodeposition of zinc-based composite coatings report that during the process, some unexpected compositions could be generated [6]. This phenomenon is due to simultaneous reactions that occur, particularly hydrogen evolution. The pH value locally changes by means of the production of hydrogen; consequently, the precipitation of $Zn(OH)_2$ and/or ZnO takes place [31].

The co-deposition of TiO_2 obviously affects the relative intensity corresponding to different crystal planes. The presence of TiO_2 in the Zn-HA coating decreases the relative intensity corresponding to the (1 0 1) crystal plane. The low intensity of the TiO_2 and HA phases, in comparison to the Zn peaks, could be attributed to the high amount of Zn in comparison to the TiO_2 and HA particles. Also, Zn with a strong ability to be detected in XRD, essentially exhibits considerable peak intensities. The NiTi peak appearing at 38.8˚ regards to its (110) plane which overlaps with the (100) plane of zinc. The crystallite size of the composite coatings was calculated by the Scherrer equation using the Full width at half maximum (FWHM) of the prominent (101) reflection. In the case of Zn-HA, the crystalline size is 53.3 nm, whereas it is 36.7 nm for the Zn-HA-TiO_2 coating. The addition of the TiO_2 nanoparticles results in the increase of sites for nucleation of Zn crystallites, so that a reduction of the crystallite size takes place [23]. It has been recognized that the structure and grain size of an electrodeposited film are determined by the rate of nucleation and crystal growth. The presence of nanoparticles provides more nucleation sites by increasing the surface area of the cathode and thus prohibits Zn growth [23,24]. The restriction of continuous growth of Zn grains have been attributed to several factors, such as: (i) the

This is the accepted manuscript (postprint) of the following article:
M. Mirak, M. Alizadeh, E. Salahinejad, R. Amini, *Zn–HA–TiO_2 nanocomposite coatings electrodeposited on a NiTi shape memory alloy*, Surface and Interface Analysis, 47 (2015) 176-183.
https://doi.org/10.1002/sia.5678

increase of the numbers of nucleation sites, (ii) the retardation of the growth of Zn grains, and (iii) changes in preferred growth orientations of grains [28].

3.2. SEM studies

Fig. 2 shows the surface morphology of the Zn-HA nanocomposite coating in two different magnifications. The SEM images reveal that the Zn-HA coating consists of a porous structure having clusters in various dimensions (Fig. 2b). As can be seen from this figure, the morphology of the Zn-HA composite coating is fine and the coating has a protruding surface. The surface morphology of the Zn-HA-TiO_2 nanocomposite coatings with two different particle contents (10 and 25 g l^{-1}) and two magnifications is shown in Fig. 3. As it can be seen, the morphology of the Zn-HA coating significantly changes after the addition of the TiO_2 nanoparticles. The morphology of the Zn-HA-TiO_2 nanocomposite coatings is more uniform and characterized by a refined surface structure at both 10 and 25 g l^{-1}. As it can be seen from Fig. 3, the addition of the TiO_2 nanoparticles improves the uniformity of the coating, which is more specified at the low magnification photo. As it is shown in the SEM surface micrographs, the porosities which are found in the Zn-HA deposited layer has remained in the Zn-HA-TiO_2 nanocomposite coatings. The adjacent lump part is adjoined together on one joint and subsequently creates a microporous structure, where the porosities are estimated to be 10 μm in diameter. Other studies conducted on electrodeposition of composite coatings with NiTi substrates, report that porous surface morphologies are promoted by the use of porous substrates [32]. According to Fig. 3d, the Zn-HA-TiO_2 coating morphology at 25 g l^{-1} consists of two distinguished parts. One part of morphology consists of plate-like regions which grow outward. The size of these plates was measured to be approximately 2 μm, developed perpendicularly to the substrate, which is in good agreement

This is the accepted manuscript (postprint) of the following article:
M. Mirak, M. Alizadeh, E. Salahinejad, R. Amini, *Zn–HA–TiO_2 nanocomposite coatings electrodeposited on a NiTi shape memory alloy*, Surface and Interface Analysis, 47 (2015) 176-183.
https://doi.org/10.1002/sia.5678

with the report of Guan et al. [7]. This plate-like structure may be favorable for bone growth, whereas apatite in bone has a plate-shaped morphology with a thickness of 2–3 nm and tens of nanometers in length and width [7]. The second part is the compact portion of the coating that comprises packed crystals (Fig. 3d).

Fig. 4 shows the side view morphology of the Zn-HA-TiO_2 coatings at 10 and 25 g l^{-1}. As it can be seen, the coatings are rough in the surface layer and porosities are seen in the inner layer, as shown by arrows. As expected, the increase of the nanoparticle contents in the coating enhances the surface roughness. The Zn-HA-TiO_2 composite coating with 25 g l^{-1} indicates a more uneven surface in comparison to the Zn-HA-TiO_2 composite coating with 10 g l^{-1}, which is related to haphazard growing path.

The typical EDX analysis related to the Zn-HA and Zn-HA-TiO_2nanocomposite coatings at 25 g l^{-1} is depicted in Fig. 5. The peaks located at 0.21, 3.7, and 4.8 keV are attributed to O, Ca and Ti, respectively. The existence of Ca and P in the form of hydroxyapatite was confirmed by the presence of HA peaks in the XRD pattern.

The HA and TiO_2 contents deposited in the coatings were measured by the EDX analysis, as depicted in Fig. 6. Each point of the figure has been extracted from the average value of five measurements at different locations on each coated sample. According to Fig. 6, the total HA andTiO_2 contents in the co-deposited Zn-HA-TiO_2 coating were more than the HA content in the Zn-HA coating at the same particle content in the electrolyte. The particle content for the Zn-HA nanocomposite coating was found to be 12.4 wt%, whereas it was 20.6 wt% for the Zn-HA-TiO_2coating. The way that the dispersed HA and TiO_2particles with zinc ions were adsorbed to the NiTi substrate is that the particles carried a net positive charge which accelerates their migration towards the negatively charged NiTi substrate surface. Also, it should be noted that if the saturation of the HA and TiO_2 particles in the composite

This is the accepted manuscript (postprint) of the following article:
M. Mirak, M. Alizadeh, E. Salahinejad, R. Amini, *Zn–HA–TiO_2 nanocomposite coatings electrodeposited on a NiTi shape memory alloy*, Surface and Interface Analysis, 47 (2015) 176-183.
https://doi.org/10.1002/sia.5678

coating happens, the screening effect of the composite coating may occur, which is related to the weakening of the electrostatic attraction between the substrate and suspended particles in the bath. In the case of the Zn-HA-TiO_2 coating, owing to the presence of the two types of ceramic particles, the saturation of the Zn matrix is postponed [29].

The elemental distribution maps of the Zn-HA and Zn-HA-TiO_2 nanocomposite coatings at 25 g l^{-1} nanoparticles made by EDX on the surface of the coatings and the corresponded micrographs are shown in Fig. 7. The surface image of the Zn-HA coating (Fig. 7a) indicates a homogenous dispersion of the particles. As it can be seen, the Zn matrix almost covers the surface and the HA particles are randomly scattered in the matrix, as is significantly visible in Fig.7a. Comparing the secondary electron (SE) image and elemental map analysis, it can be possible to locate HA particles, as shown by arrows. Fig. 7b indicates the SE image and X-ray mapping of the individual elements of the plate-like section of the Zn-HA-TiO_2 coating, showing a uniform distribution of the elements in the coating. The plate-like portion mainly consists of HA. The individual elements of Ca and P show that HA is completely dispersed over the section, like the Zn matrix, but with a less intensity. Furthermore, the TiO_2 nanoparticles are seen and no agglomeration of the nanoparticles is observed.

The line scan profile across the Zn-HA-TiO_2 nanocomposite coating at 25 g l^{-1} is shown in Fig. 8. It indicates that the coating layer consists of Zn, Ca, P and Ti. As it can be seen, the content of the elements changes from the interface to the coating surface. The intensity of the Zn K_α line possesses its maximum value at the beginning of co-deposition, and by progression of the electrodeposition process it decreases, while the intensity of the Ca, P and Ti K_α lines increases with increasing the coating thickness, so that their maximum values are attained at the end ofthe process. The high amount of Ti peaks at the initiation of scan is

This is the accepted manuscript (postprint) of the following article:
M. Mirak, M. Alizadeh, E. Salahinejad, R. Amini, *Zn–HA–TiO_2 nanocomposite coatings electrodeposited on a NiTi shape memory alloy*, Surface and Interface Analysis, 47 (2015) 176-183.
https://doi.org/10.1002/sia.5678

related to the substrate. The increase of the particles peaks by progression of the process could be explained in terms of electrostatic interactions between the electrode and ceramic particles. At the beginning of the electrodeposition, the main reaction at the surface of the cathode is the deposition of zinc [18], due to the high reduction capacity of Zn [8], whereas a few contents of the HA and TiO_2 particles are placed on the deposit, due to the poor electrostatic attraction between the particles and cathode surface. By increasing the coating thickness, the content of Zn decreased, due to the significant hydrogen evolution, which results in Zn hydration at the metal-solution interface and the decrease of the Zn deposition efficiency [9]. Moreover, the electrophoretic migration of the HA and TiO_2 particles which is related to electrostatic forces between the particles and cathode remains almost constant [22]. Therefore, the deposition of the HA and TiO_2 particles is nearly not influenced.

3.3. TEM observation

Fig. 9 indicates the HRTEM image and the corresponding EDX pattern of two different typical spots in the nanocrystalline Zn–HA-TiO_2 specimen produced at 25 g l^{-1} nanoparticles. As shown, the EDX analyses fairly confirm the chemical composition of the Zn matrix and an HA particle of approximately 60 nm in size. Good adhesion between the matrix and reinforcement in the coating is also noticeable, as observed in the micrograph.

3.4. Effect of the particle concentration on microhardness

The microhardness of the Zn–HA-TiO_2 nanocomposite coating at different particle contents in the electrolyte is shown in Fig. 10. As it can be seen, the microhardness of the Zn deposit is about 95 HV. However, with the addition of the nanoparticles, the microhardness of the Zn–HA-TiO_2 nanocomposite is significantly increased. The microhardness of the Zn–

This is the accepted manuscript (postprint) of the following article:
M. Mirak, M. Alizadeh, E. Salahinejad, R. Amini, *Zn–HA–TiO_2 nanocomposite coatings electrodeposited on a NiTi shape memory alloy*, Surface and Interface Analysis, 47 (2015) 176-183.
https://doi.org/10.1002/sia.5678

HA-TiO_2 nanocomposite coatings increases with increasing the nanoparticle content and reach 420 HV at 25 g l^{-1}. The increase of hardness can be explained by a decrease of the zinc crystallite size, due to the embedding of the nanoparticles in the coating, which is represented by the Hall–Petch equation:

$$HV = H_0 + kd^{-1/2} \quad (1)$$

where *HV* is the measured hardness, H_0 and *k* are constants, and *d* is the average crystallite size. According to the equation, grain boundaries behave as barriers against the motion of dislocations by forming dislocation pile-ups at grain boundaries, resulting in hard deposits. Also, the enhancement in hardness might be caused by strength hardening of incorporated nanoparticles in the Zn matrix, which inhibits the plastic flow of the metal [34].

3.5. Effect of the particle concentration on wear properties

Fig. 11 shows the dependence of the wear weight loss as a function of distance for 5 and 25 g l^{-1} in the electrolyte bath. As it is evident from this figure, the wear of the deposits increases with increasing the distance, while the wear resistance of the composite coating at 25 g l^{-1} is higher than that of 5 g l^{-1}. This behavior is due to the more incorporation of the hard TiO_2 nanoparticles in the coating, which carries loads applied on the matrix; as a result, it not only prevents thermal plastic deformation, but also reduces scuffing wear at high temperatures caused by the heat generation during friction. From the initial stage of the wear test, a difference in the wear rate of both of the composite coatings is observed, so that this difference increases at the last 50 m distance. It is suggested that in this particular case, the detachment of wear debris occurs as a result of the past wear process. This wear debris acts as abrasive particles trapped between the ball and coating surface, and intensifies the weight loss of the coating [35]. Hence, the 5 g l^{-1} nanocomposite coating is unable to bear this condition,

This is the accepted manuscript (postprint) of the following article:
M. Mirak, M. Alizadeh, E. Salahinejad, R. Amini, *Zn–HA–TiO_2 nanocomposite coatings electrodeposited on a NiTi shape memory alloy*, Surface and Interface Analysis, 47 (2015) 176-183.
https://doi.org/10.1002/sia.5678

so that an increase in the weight loss of the coating is observed. However, the 25 g l^{-1} nanocomposite coating efficiently resists under these specific testing conditions.

4. Conclusions

In the present study, Zn-HA and Zn-HA-TiO_2 nanocomposite coatings were prepared by co-electrodeposition on a NiTi substrate. The structural and mechanical properties of the nanocomposite coatings were evaluated. The following conclusions were obtained:

1) The addition of 25 g l^{-1} of the HA and TiO_2 nanoparticles to the Zn matrix affected the microstructure of the coating and changed the morphology to a plate–like crystallite feature.

2) The weight percent of the particles deposited in the Zn-HA-TiO_2 composite coating was more than that of the Zn-HA composite coating at the same particle content in the electrolyte bath.

3) The elemental mapping on the Zn-HA-TiO_2 surface showed that the HA and TiO_2 nanoparticles were homogeneously distributed in the Zn matrix.

4) By progression of the electrodeposition process, the amount of the particles across the coating section was increased.

5) The coatings reinforced with the nanoparticles yielded the microhardness values as high as 420 HV at 25 g l^{-1} because of the unique dispersion effect, whereas the microhardness of the unreinforced Zn matrix was 95 HV.

6) The Zn-HA-TiO_2 nanocomposite coating at 25 g l^{-1}exhibited a better wear resistance compared to the same composite coating at 5 g l^{-1}.

5. Acknowledgement

This is the accepted manuscript (postprint) of the following article:
M. Mirak, M. Alizadeh, E. Salahinejad, R. Amini, *Zn–HA–TiO_2 nanocomposite coatings electrodeposited on a NiTi shape memory alloy*, Surface and Interface Analysis, 47 (2015) 176-183.
https://doi.org/10.1002/sia.5678

The authors would like to thank the Shiraz University of technology (Department of Materials Science and Engineering) for the support of this study.

References

[1] J. Ryhänen, M. Kallioinen, J. Tuukkanen, P. Lehenkari, J. Junila, E. Niemelä, P.Sandvik, W. Serlo, *Biomater.* **1999**; *20*, 1309.

[2] G. Rondelli, B. Vicentini, *Biomater.* **1999**; *20*, 785.

[3] D.J. Wever, A.G. Veldhuizen, J. de Vries, H.J. Busscher, D.R.A. Uges, J.R. van Horn, *Biomater.* **1998**; *19*, 761.

[4] W. Suchaneck, M. Yoshimura, *J. Mater. Res.* **1998**; *13*, 94.

[5] B.M. Praveen, T.V. Venkatesha, *Appl. Surf. Sci.* **2008**; *254*, 2418.

[6] T. Frade, V. Bouzon, A. Gomes, M.I. da Silva Pereira, *Surf. Coat. Tech.* **2010**; *204*, 3592.

[7] H.X. Wang, S.K. Guan, X. Wang, C.X. Ren, L.G. Wang, *Acta Biomater.* **2010**; *6*, 1743.

[8] W. Xu, W. Hu, M. Li, Q. Ma, P.D. Hodgson, C. Wen, *T. Nonferr. Metal. Soc.* **2006**; *16*, 209.

[9] Y. Tang, H. F. Chappell, M. T. Dove, R. J. Reeder, Y. J. Lee, *Biomater.* **2009**; *30*, 2864.

[10] H. Li, K.A. Khor, P. Cheang, *Biomater.* **2003**; *24*, 949.

[11] J.M. Zhang, C.J. Lin, Z.D. Feng, Z.W. Tian, *J. Electroanal. Chem.* **1998**; *452*, 235.

[12] Q. Li, X. Yang, L. Zhang, J. Wang, B. Chen, *J. Alloys Compd.* **2009**; *482*, 339.

[13] J. Takebe, S. Itoh, J. Okada, K. Ishibashi, *J. Biomed. Mater. Res.* **2000**; *51*, 398.

[14] K.S. Raja, M. Misra, K. Paramguru, *Mater. Lett.* **2005**; *59*, 2137.

[15] L. Mohan, D. Durgalakshmi, M. Geetha, T.S.N. Sankara Narayanan, R. Asokamani, *Ceram. Int.* **2012**; *38*, 3435.

[16] M. Jarcho, *Clin. Orthop. Relat. Res.* **1981**; *157*, 259.

This is the accepted manuscript (postprint) of the following article:
M. Mirak, M. Alizadeh, E. Salahinejad, R. Amini, *Zn–HA–TiO_2 nanocomposite coatings electrodeposited on a NiTi shape memory alloy*, Surface and Interface Analysis, 47 (2015) 176-183.
https://doi.org/10.1002/sia.5678

[17] S.D. Cook, K.A. Thomas, J.F. Kay, M. Jarcho, *Clin. Orthop. Relat. Res.* **1988**; *232*, 225.

[18] V. Nelea, C. Ristoscu, C. Chiritescu, C. Ghica, I.N. Mihailescu, H. Pelletier, P. Mille, A. Cornet, *Appl. Surf. Sci.* **2000**; *168*,127.

[19] M. Inagaki, Y. Yokogawa, T. Kameyama, *Thin Solid Films* **2001**; *386*, 222.

[20] K. Cheng, C. Ren, W. Weng, P. Du, G. Shen, G. Han, S. Zhang, *Thin Solid Films* **2009**; *517*, 5361.

[21] Y.C. Yang, E. Chang, *Biomater.* **2001**; *22*, 1827.

[22] A. J. Nathanael, N. S. Arul, N. Ponpandian, D. Mangalaraj, P.C. Chen, *Thin Solid Films* **2010**; *518*, 7333.

[23] M.R. Vaezi, S.K. Sadrnezhaad, L. Nikzad, *Coll. and Surf. A: Physicochem. Eng. Aspects* **2008**; *315*, 176.

[24] L. Benea, P.L. Bonora, A. Borello, S. Martelli, F. Wenger, P. Ponthiaux, J. Galland, *Solid State Ionics* **2002**; *151*, 89.

[25] M. Srivastava, J.N. Balaraju, B. Ravishankar, K.S. Rajam, *Surf. Coat. Tech.* **2010**; *205*, 66.

[26] T. Lampke, B. Wielage, D. Dietrich, A. Leopold, *Appl. Surf. Sci.* **2006**; *253*, 2399.

[27] A.D. Pogrebnjak, Sh.M. Ruzimov, D.L. Alontseva, P. Zukowski, C. Karwat, C. Kozak, M. Kolasik, *Vacuum* **2007**; *81*, 1243.

[28] B. Scharifker, G. Hills, *Electrochim. Acta* **1983**; *28*, 879.

[29] I. ul Haq, T. I. Khan, *Surf. Coat. Tech.* **2011**; *205*, 2871.

[30] X. Liu, P. Chu, C. Ding, *Mater. Sci. Eng R.* **2004**; *47*, 49.

[31] A. Gomes, M.I. da Silva Pereira, *Electrochim. Acta* **2006**; *52*, 863.

[32] O. Prymaka, D. Bogdanskib, M. Ko¨ llerb, S. A. Esenweinb, G. Muhrb, F. Beckmannc, T. Donathc, M. Assadd, M. Epple, *Biomater.* **2005**; *26*, 5801.

This is the accepted manuscript (postprint) of the following article:
M. Mirak, M. Alizadeh, E. Salahinejad, R. Amini, *Zn–HA–TiO_2 nanocomposite coatings electrodeposited on a NiTi shape memory alloy*, Surface and Interface Analysis, 47 (2015) 176-183.
https://doi.org/10.1002/sia.5678

[34] I. Garcia, J. Fransaer, J. P. Celis, *Surf. Coat. Tech.* **2001**; *148*, 171.

[35] E.E. Vera, M. Vite, R. Lewis, E.A. Gallardo, J.R. Laguna-Camacho, *Wear* **2011**; *271*, 2116.

This is the accepted manuscript (postprint) of the following article:
M. Mirak, M. Alizadeh, E. Salahinejad, R. Amini, *Zn–HA–TiO_2 nanocomposite coatings electrodeposited on a NiTi shape memory alloy*, Surface and Interface Analysis, 47 (2015) 176-183.
https://doi.org/10.1002/sia.5678

Figures:

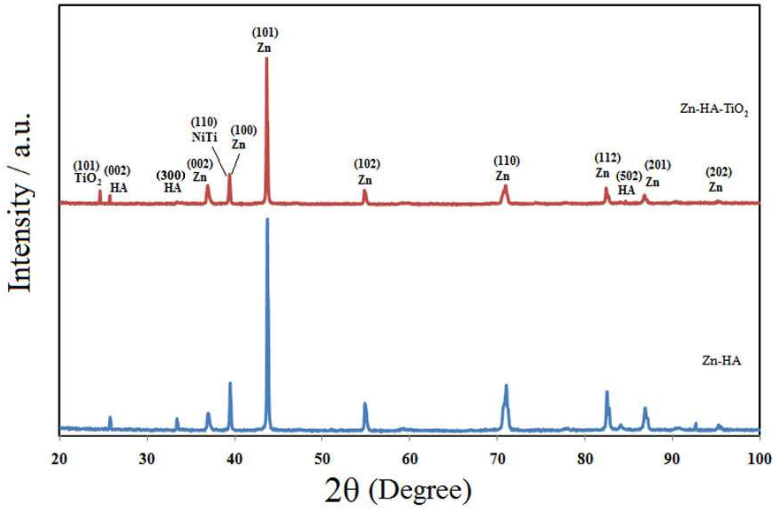

Fig. 1. XRD patterns of the Zn-HA and Zn-HA-TiO_2 coatings deposited at a current density of 1 Adm^{-2}.

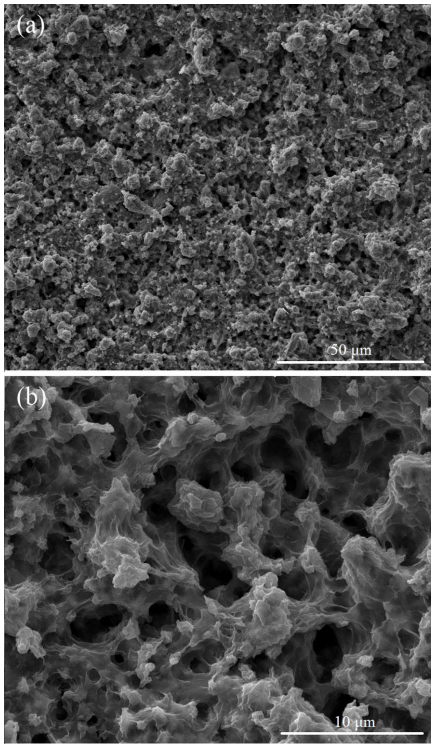

Fig. 2. SEM micrograph of the Zn-HA coating in two magnifications (a and b).

This is the accepted manuscript (postprint) of the following article:
M. Mirak, M. Alizadeh, E. Salahinejad, R. Amini, *Zn–HA–TiO_2 nanocomposite coatings electrodeposited on a NiTi shape memory alloy*, Surface and Interface Analysis, 47 (2015) 176-183.
https://doi.org/10.1002/sia.5678

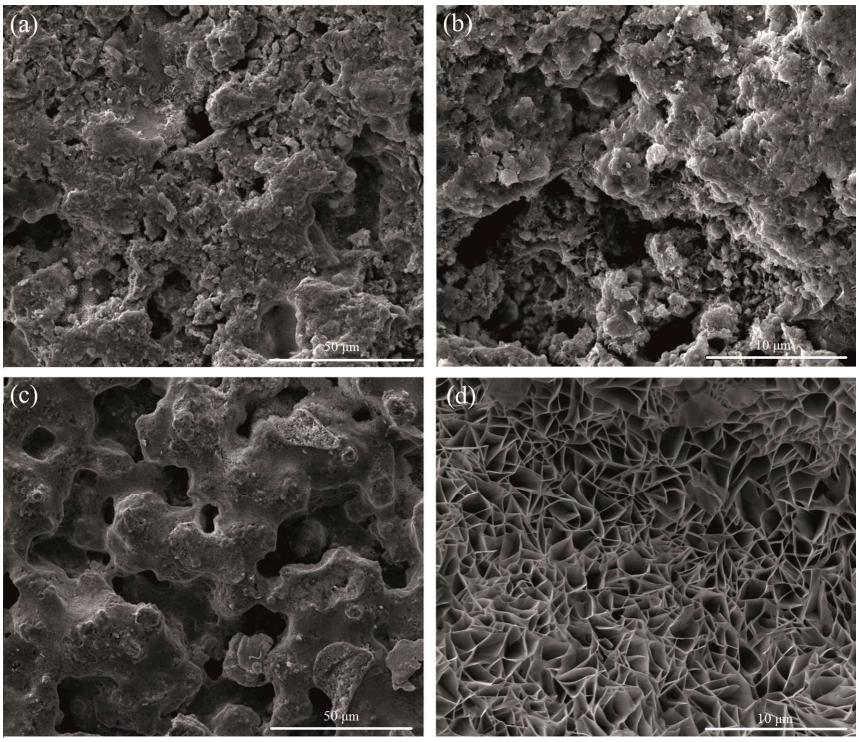

Fig. 3. SEM micrograph of the Zn-HA-TiO_2 coatings with the particle contents of 10 g l^{-1} (a and b) and 25 g l^{-1} (c and d) in two magnifications.

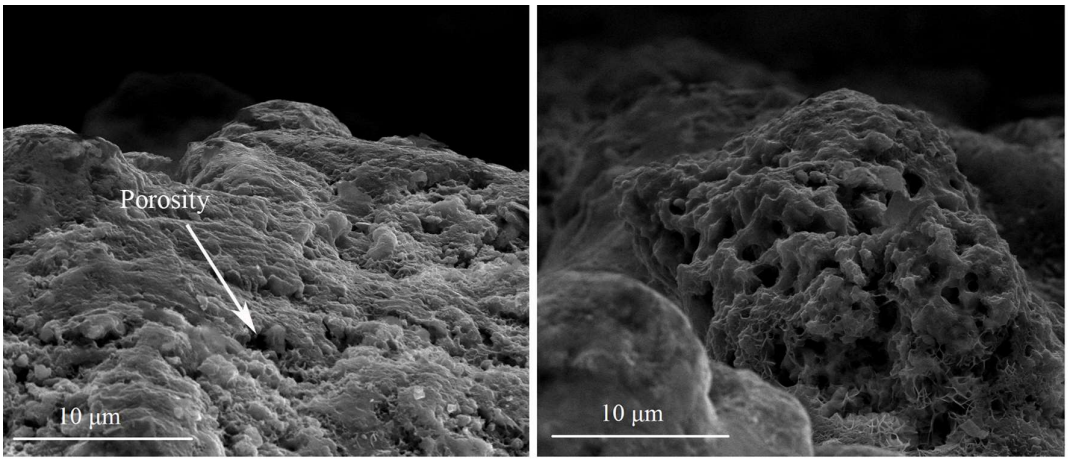

Fig. 4. Side-view SEM micrograph of the Zn-HA-TiO_2 coatings deposited at 10 g l^{-1} (a) and 25 g l^{-1} (b).

This is the accepted manuscript (postprint) of the following article:
M. Mirak, M. Alizadeh, E. Salahinejad, R. Amini, *Zn–HA–TiO_2 nanocomposite coatings electrodeposited on a NiTi shape memory alloy*, Surface and Interface Analysis, 47 (2015) 176-183.
https://doi.org/10.1002/sia.5678

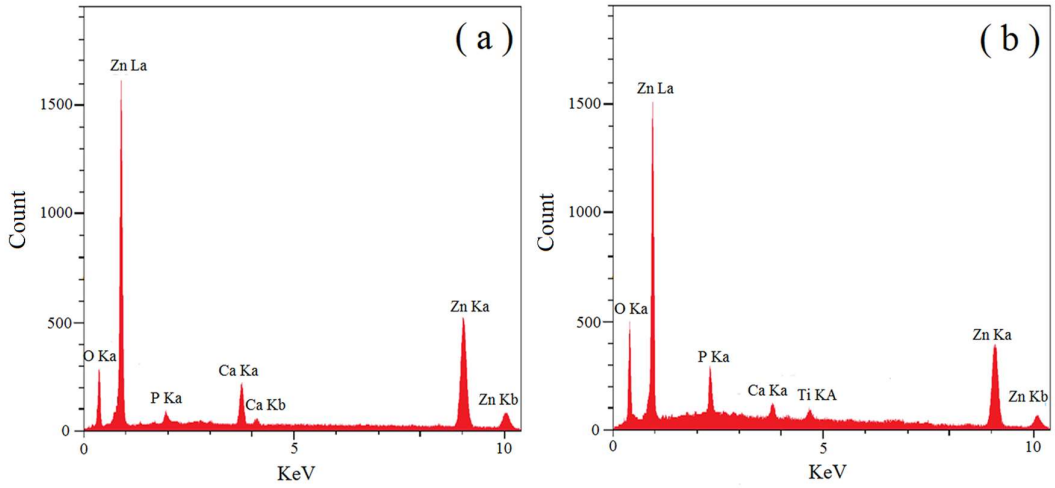

Fig. 5. EDX analyses related to the Zn-HA (a) and Zn-HA-TiO_2 (b) coatings deposited at 25 g l^{-1}.

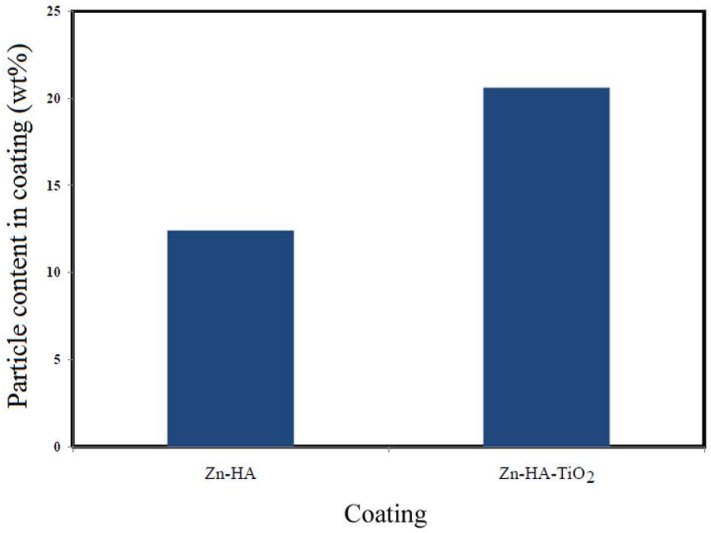

Fig. 6. Particle contents deposited in the coatings, measured by the EDX analysis.

This is the accepted manuscript (postprint) of the following article:
M. Mirak, M. Alizadeh, E. Salahinejad, R. Amini, *Zn–HA–TiO_2 nanocomposite coatings electrodeposited on a NiTi shape memory alloy*, Surface and Interface Analysis, 47 (2015) 176-183.
https://doi.org/10.1002/sia.5678

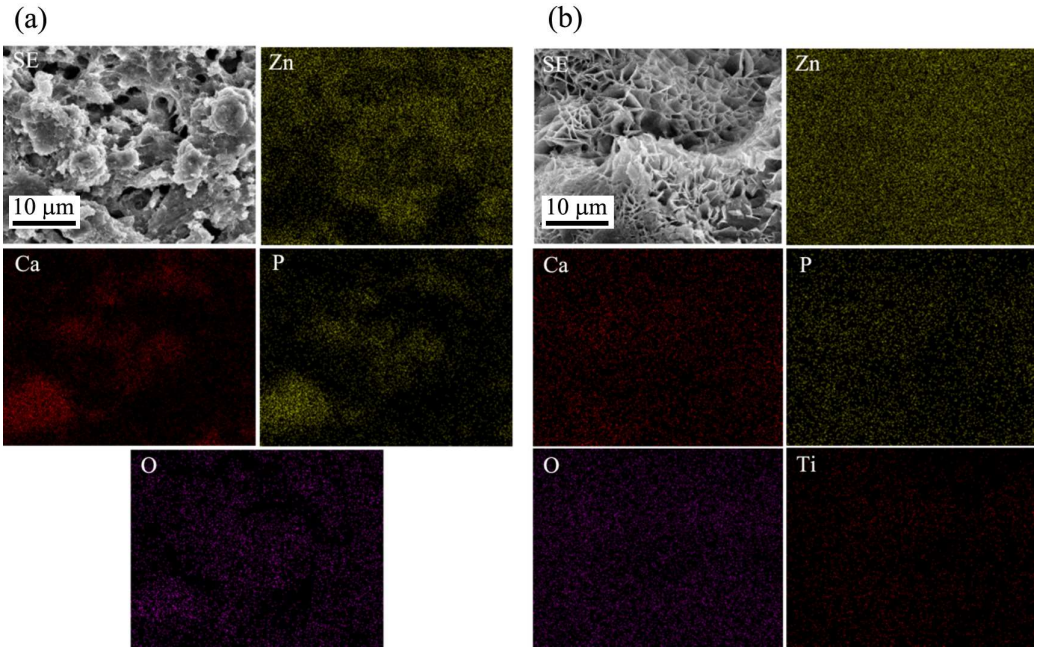

Fig. 7. Micrographs and elemental distribution maps of the Zn-HA (a) and Zn-HA-TiO_2 (b) coatings deposited at 25 g l^{-1} nanoparticles.

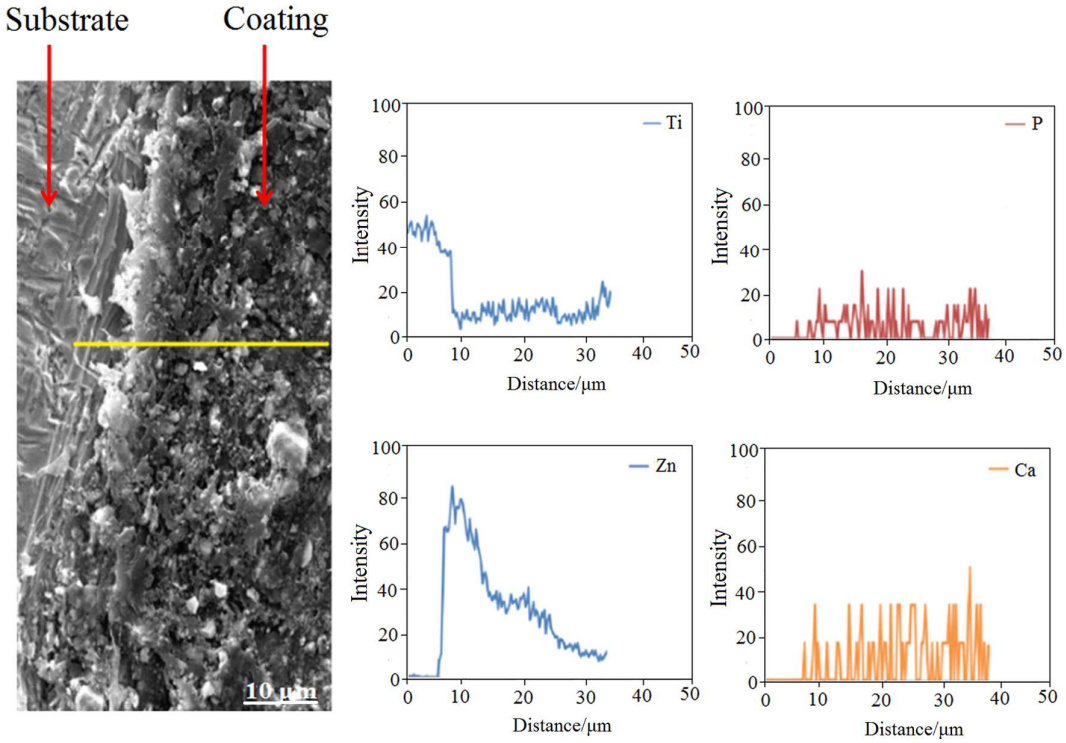

Fig. 8. Line scan profile across the Zn-HA-TiO_2 nanocomposite coating deposited at 25 g l^{-1}.

This is the accepted manuscript (postprint) of the following article:
M. Mirak, M. Alizadeh, E. Salahinejad, R. Amini, *Zn–HA–TiO_2 nanocomposite coatings electrodeposited on a NiTi shape memory alloy*, Surface and Interface Analysis, 47 (2015) 176-183.
https://doi.org/10.1002/sia.5678

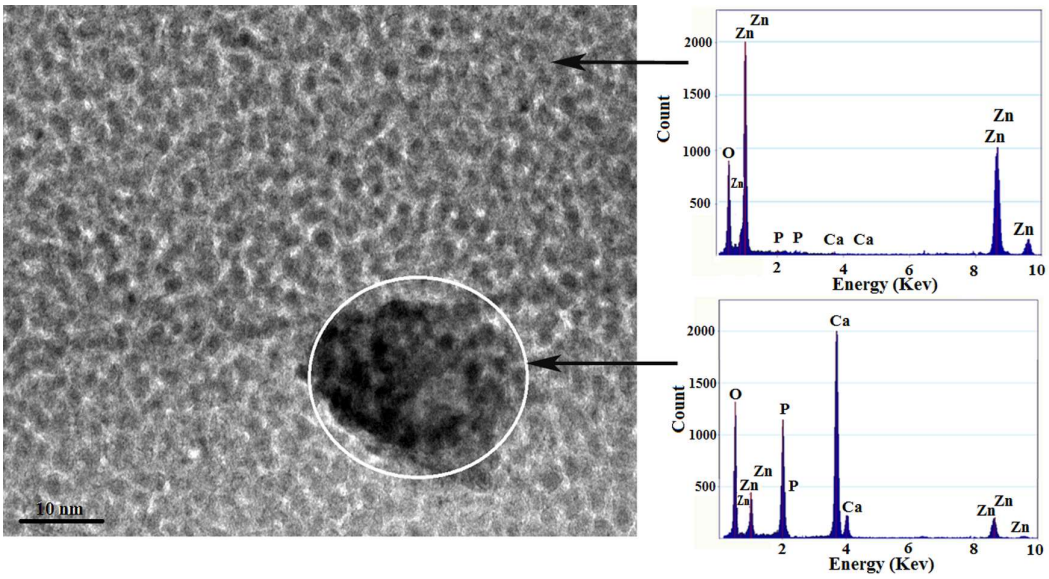

Fig. 9. HRTEM and corresponding EDX pattern of two different typical spots for the Zn–HA-TiO_2 specimen produced at 25 g l^{-1}.

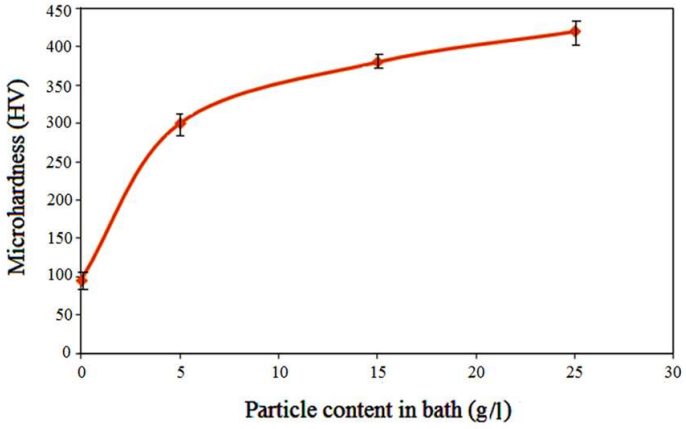

Fig. 10. Microhardness of the Zn–HA-TiO_2 coating at the different particle contents in the electrolyte.

This is the accepted manuscript (postprint) of the following article:
M. Mirak, M. Alizadeh, E. Salahinejad, R. Amini, *Zn–HA–TiO_2 nanocomposite coatings electrodeposited on a NiTi shape memory alloy*, Surface and Interface Analysis, 47 (2015) 176-183.
https://doi.org/10.1002/sia.5678

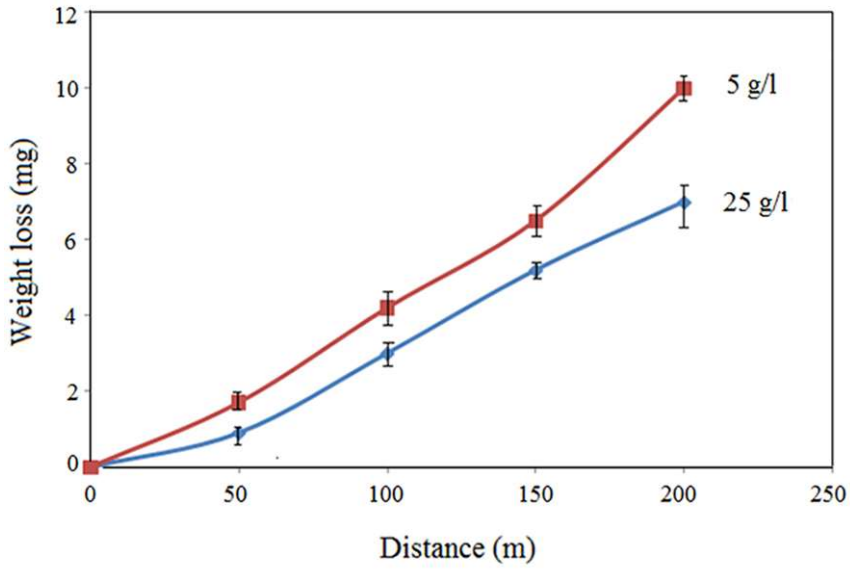

Fig. 11. Wear weight loss as a function of distance for 5 and 25 g l^{-1} in the electrolyte bath.

This is the accepted manuscript (postprint) of the following article:
M. Mirak, M. Alizadeh, E. Salahinejad, R. Amini, *Zn–HA–TiO_2 nanocomposite coatings electrodeposited on a NiTi shape memory alloy*, Surface and Interface Analysis, 47 (2015) 176-183.
https://doi.org/10.1002/sia.5678

Table:

Table 1. Chemical composition of the bath and conditions of electrodeposition.

Bath composition	Concentration (gl^{-1})	Parameters
$ZnCl_2$	15	Current density: 1 A dm^{-2}
NH_4Cl	120	Temperature: 25±1 °C
Saccharin	5	pH: 3.7±0.2
$C_{12}H_{25}NaO_4S$ (SDS)	0.4	Stirring rate: 150 rpm
HA particle	0-25	
TiO_2 particle	0-12.5	